Article

Amycolachromones A–F, Isolated from a Streptomycin-Resistant Strain of the Deep-Sea Marine Actinomycete *Amycolatopsis* sp. WP1

Jianwei Chen [1,†]**, Jun Chen** [2,†]**, Siqi Wang** [1]**, Xiaoze Bao** [1]**, Songwei Li** [1]**, Bin Wei** [1]**, Huawei Zhang** [1] **and Hong Wang** [1,3,]*

1   College of Pharmaceutical Science & Collaborative Innovation Center of Yangtze River Delta Region Green Pharmaceuticals, Zhejiang University of Technology, Hangzhou 310014, China; cjw983617@zjut.edu.cn (J.C.); 2112007272@zjut.edu.cn (S.W.); baoxiaoze@zjut.edu.cn (X.B.); songweili93@zjut.edu.cn (S.L.); binwei@zjut.edu.cn (B.W.); hwzhang@zjut.edu.cn (H.Z.)
2   College of Biotechnology and Pharmaceutical Engineering, West Anhui University, Lu'an 237499, China; 02000179@wxc.edu.cn
3   Key Laboratory of Marine Fishery Resources Exploitment and Utilization of Zhejiang Province, Zhejiang University of Technology, Hangzhou 310014, China
*   Correspondence: hongw@zjut.edu.cn; Tel.: +86-0571-8832-0622
†   These authors contributed equally to this work.

Abstract: In this study, a detailed chemical investigation of a streptomycin-resistant strain of the deep-sea marine, actinomycete *Amycolatopsis* sp. WP1, yielded six novel amycolachromones A–F (**1**–**6**), together with five known analogues (**7**–**11**). Amycolachromones A–B (**1**–**2**) possessed unique dimer skeletons. The structures and relative configurations of compounds **1**–**11** were elucidated by extensive spectroscopic data analyses combined with X-ray crystal diffraction analysis. Plausible biogenetic pathways of amycolachromones A–F were also proposed.

1. Introduction

Marine microbial natural products, especially those derived from marine actinomycetes, have become an important source of novel bioactive compounds [1–3]. However, traditional screening strategies generally do not provide access to the full array of secondary metabolites encoded within actinomycete genomes [4]. For example, *Streptomyces coelicolor* initially produces four classes of metabolites using laboratory fermentation, despite genome sequencing revealing the capacity to produce >30 families of metabolites [5,6]. To solve this problem, various strategies have been proposed to activate the expression of otherwise silent biosynthetic gene clusters, including the 'one strain many compounds' (OSMAC) approach [7], co-cultivation with other microorganisms [8] and chemical epigenetics [9]. Recently, a ribosome engineering approach that targets ribosomal proteins or RNA polymerase (RNAP) has shown promise for expression of cryptic gene clusters. This method selects for mutants that are resistant to antibiotics that target the bacterial ribosome, presumably activating the expression of bacterial cryptic genes by resistant mutants [10,11]. Shima and co-workers demonstrated this method in actinomycetes by activating the biosynthetic pathway for actinorhodin in mutant Streptomyces that developed resistance to streptomycin [12]. Recent adoptions of this approach demonstrated the ability of streptomycin-resistant mutants to enhance production of actinolactomycin [13], fredericamycin A and chlorinated alkaloids, inducamides A–C [14,15].

Chromones are oxygen-containing heterocyclic compounds with a chromone benzoannelated γ-pyrone ring (4H-chromen-4-one, 4H-1-benzopyran-4-one) that are widely distributed in bacteria, fungi and plant [16]. Chromones and analogues can be considered

privileged structures in drug discovery due to their numerous biological activities, such as anti-inflammatory, antiplatelet, anticancer, antimicrobial, anti-neurodegenerative and anti-obesity effects [17]. In this paper, we undertook a ribosome engineering approach for activating biosynthetic pathways in *Amycolatopsis* sp. WP1, a deep sea actinomycete isolated from sediments collected at −2945 m in the Indian Ocean. A streptomycin-resistant strain, designated as L-30-6 (Figure 1), was observed to produce six new chromone derivatives, designated as the amycolachromones A–F (**1**–**6**), and five known chromone derivatives (**7**–**11**) (Figure 2).
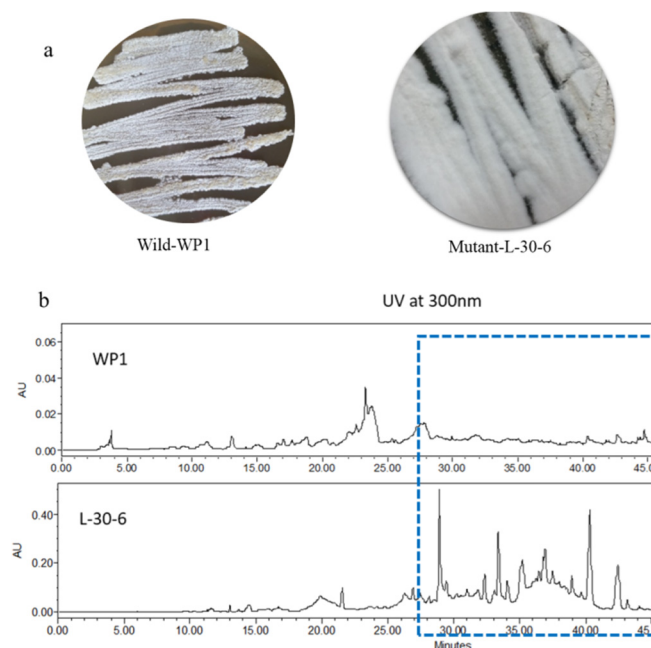

Figure 1. (**a**) Wild-type strain WP1 and streptomycin-resistant strain L-30-6 grown under identical conditions on ISP$_2$ media. (**b**) HPLC traces of wt-WP1 and mutant L-30-6 showing the production of new compounds (UV detection at 300 nm).
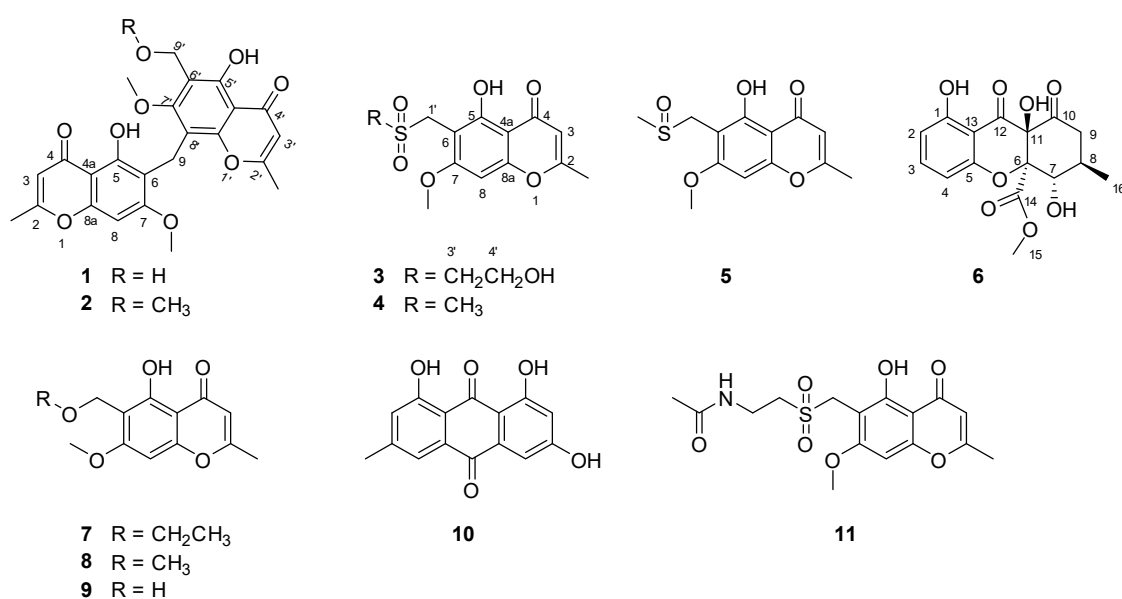

Figure 2. Chemical structures of compounds **1**–**11**.

2. Results and Discussion

Amycolachromone A (**1**) displayed HRESIMS peak at m/z 477.1172 [M + Na]$^+$ (calcd 477.1162) corresponding to the molecular formula $C_{24}H_{22}O_9$, indicating fourteen degrees of unsaturation. Analysis of the NMR data of **1** (Table 1, see Supplementary Materials) revealed three aromatic protons at δ_H 6.64 (1H, s, H-8), 6.22 (1H, s, H-3′), 6.20 (1H, s, H-3), two methoxy groups at δ_H 3.83 (3H, s, CH$_3$O-7) and 3.75 (3H, s, CH$_3$O-7′), two methyl groups at δ_H 2.35 (3H, s, CH$_3$-2) and 3.21 (3H, s, CH$_3$-2′), two methylenes at δ_H 4.45 (2H, d, J = 4.8 Hz, H-9′) and 3.98 (2H, s, H-9), two phenolic hydroxyl groups at δ_H 13.13 (1H s, OH-5) and 13.10 (1H s, OH-5′), a hydroxyl group at δ_H 4.78 (1H, t, J = 5.2 Hz, OH-9′). The ^{13}C NMR (Table 1) revealed 24 carbon signals: the two carbonyls C-4 (δ_C 183.2) and C-4′ (δ_C 182.5), the three aromatic carbons C-3 (δ_C 108.7), C-3′ (δ_C 108.4) and C-8 (δ_C 90.6), five non-oxygenated quaternary aromatic carbons at C-4a (δ_C 110.8), C-6 (δ_C 104.4), C-4a′ (δ_C 106.7), C-6′ (δ_C 117.6), and C-8′ (δ_C 112.5), eight oxygenated quaternary aromatic carbons at C-2 (δ_C 168.5), C-2′ (δ_C 168.3), C-7 (δ_C 163.8), C-7′ (δ_C 163.5), C-5 (δ_C 158.5), C-5′ (δ_C 158.3), C-8a (δ_C 156.7), and C-8a′ (δ_C 154.8), two methoxy groups CH$_3$O-7 (δ_C 63.2) and CH$_3$O-7′ (δ_C 56.7), two methyl groups CH$_3$-2 (δ_C 20.4) and CH$_3$-2′ (δ_C 20.0), and two methylenes C-9′ (δ_C 52.1) and C-9 (δ_C 16.9). Analysis of the ^{1}H and ^{13}C NMR data of **1** revealed the presence of the same 5-hydroxy-4H-chromen-4-one moiety as found in xanthones [18,19], and therefore suggested a compound comprising two xanthone building blocks.

Table 1. ^{1}H (500 MHz) and ^{13}C (125 MHz) NMR data of compounds **1** and **2** in DMSO-d_6.

Position	1		2	
	δ_H	δ_C, Type	δ_H	δ_C, Type
2		168.5, C		168.8, C
3	6.22 (s, 1H)	108.7, CH	6.23 (s, 1H)	108.7, CH
4		183.2, C		183.2, C
4a		110.8, C		110.8, C
5		158.5, C		158.9, C
6		104.4, C		100.9, C
7		163.8, C		164.2, C
8	6.64 (s, 1H)	90.6, CH	6.63 (s, 1H)	90.6, CH
8a		156.7, C		156.7, C
9	3.98 (s, 2H)	16.9, CH$_2$	3.98 (s, 2H)	16.9, CH$_2$
2′		168.3, C		168.2, C
3′	6.20 (s, 1H)	108.4, CH	6.22 (s, 1H)	108.5, CH
4′		182.5, C		182.4, C
4a′		106.7, C		106.7, C
5′		158.3, C		158.6, C
6′		117.6, C		114.1, C
7′		163.5, C		163.4, C
8′		112.2, C		112.5, C
8a′		154.8, C		154.8, C
9′	4.45 (d, J = 4.8 Hz, 2H)	52.1, CH$_2$	4.35 (s, 2H)	63.2, CH$_2$
2-CH$_3$	2.35 (s, 3H)	20.4, CH$_3$	2.35 (s, 3H)	20.4, CH$_3$
7-OCH$_3$	3.83 (s, 3H)	63.2, CH3	3.82 (s, 3H)	62.5, CH3
2′-CH$_3$	2.21 (s, 3H)	20.0, CH$_3$	2.21 (s, 3H)	20.0, CH$_3$
7′-OCH$_3$	3.75 (s, 3H)	56.7, CH$_3$	3.76 (s, 3H)	56.6, CH$_3$
9′-OCH$_3$			3.29 (s, 3H)	57.7, CH$_3$
5-OH	13.13 (s, 1H)		13.21 (s, 1H)	
5′-OH	13.10 (s, 1H)		13.11 (s, 1H)	
9′-OH	4.78 (t, J = 5.2 Hz, 1H)			

^{1}H-^{1}H COSY correlations were observed from H-9′ to OH-9′. Further confirmation was found for HMBC correlations of 5-OH to C-5, C-6, 4a; H-8 to C-6, C-4a, C-8a; H-3 to C-2; 2-CH$_3$ to C-2, C-3, indicating the same Eugenin. HMBC correlations from 5′-OH to C-5′, C-6′, 4a′; H-3′ to C-2′; 2′-CH$_3$ to C-2′, C-3′; H-9′ to C-5′, C-6′, C-7′, indicated the

same 6-Hydroxymethyleugenin (**10**) [20]. HMBC correlations from H-9 to C-7, C-5, C-4a, C8′, C-7, C-8a′, indicated that Eugenin and 6-hydroxymethyleugenin are linked with C-9. Selected key correlations in the observed NMR spectrum are shown in Figure 3. On the basis of these results, the structure of compound **1** was established as shown.
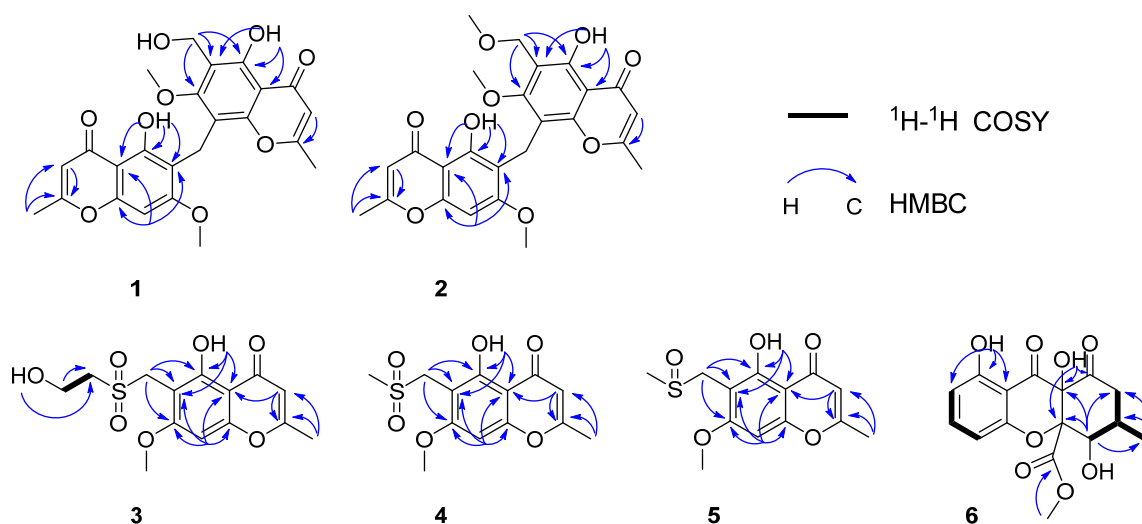

Figure 3. Key HMBC and COSY correlations of compounds **1–6**.

Amycolachromone B (**2**) displayed HRESIMS peak at *m/z* 469.1502 [M + H]⁺ (calcd 469.1499), *m/z* 491.1333 [M + Na]⁺ (calcd 469.1318), corresponding to the molecular formula $C_{25}H_{24}O_9$ (fourteen degrees of unsaturation). Analysis of the NMR data of **2** (Table 1) revealed for three aromatic protons at δ_H 6.64 (1H, s, H-8), 6.22 (1H, s, H-3′), 6.23 (1H, s, H-3), two methoxy groups at δ_H 3.82 (3H, s, CH₃O-7) and 3.76 (3H, s, CH₃O-7′), two methyl groups at δ_H 2.22 (3H, s, CH₃-2) and 3.37 (3H, s, CH₃-2′), two methylene at δ_H 4.35 (2H, s, H-9′) and 3.98 (2H, s, H-9), two phenolic hydroxyl groups at δ_H 13.21 (1H s, OH-5) and 13.11 (1H s, OH-5′). The ¹³C NMR (Table 1) revealed 25 carbon signals: the two carbonyl group C-4 (δ_C 183.2), C-4′ (δ_C 182.4), three aromatic carbon C-3 (δ_C 108.7), C-3′ (δ_C 108.5) and C-8 (δ_C 90.6), five nonoxygenated quaternary aromatic carbons at C-4a (δ_C 110.8), C-6 (δ_C 100.9), C-4a′ (δ_C 106.7), C-6′ (δ_C 114.1), and C-8′ (δ_C 112.5), eight oxygenated quaternary aromatic carbons at C-2 (δ_C 168.8), C-2′ (δ_C 168.2), C-7 (δ_C 164.2), C-7′ (δ_C 163.4), C-5 (δ_C 158.9), C-5′ (δ_C 158.6),C-8a (δ_C 156.7), and C-8a′ (δ_C 154.8), three methoxy groups CH₃O-7(δ_C 62.5), CH₃O-9′ (δ_C 57.7), and CH₃O-7′ (δ_C 56.6), two methyl groups CH₃-2 (δ_C 20.4) and CH₃-2′ (δ_C 20.0), two methylene C-9′ (δ_C 63.2) and C-9 (δ_C 16.9). Analysis of the ¹H and ¹³C NMR data of **2** revealed the presence of the same 5-hydroxy-4H-chromen-4-one moiety as found in xanthones [18,19], and comprised two xanthones. In contrast, the NMR data of **2** showed them to be nearly identical except for a methoxy group linked with C-9′. Further confirmation was found for HMBC correlations of 5-OH to C-5, C-6, 4a; H-8 to C-6, C-4a, C-8a, C-7; H-3 to C-2; 2-CH₃ to C-2, C-3, indicated that same as Eugenin [20]. HMBC correlations from 5′-OH to C-5′, C-6′, 4a′; H-3′ to C-2′; 2′-CH₃ to C-2′, C-3′; H-9′ to C-5′, C-6′, C-7′, indicated that same as 6-Methoxymethyleugenin (**9**) [21]. HMBC correlations from H-9 to C-7, C-5, C-4a, C8′, C-7, C-8a′, indicated that Eugenin and Methoxymethyleugenin are linked with C-9. Selected key correlations in the observed NMR spectrum are shown in Figure 3. On the basis of these results, the structure of compound **2** was established as shown.

Amycolachromone C (**3**) displayed HRESIMS ion at *m/z* 351.0515 [M + Na]⁺ (calcd 351.0514), corresponding to the molecular formula $C_{14}H_{16}O_7S$, indicating nine degrees of unsaturation. Analysis of the NMR data of **3** (Table 2) revealed two aromatic protons at δ_H 6.78 (1H, s, H-8), 6.32 (1H, s, H-3), a methoxy group at δ_H 3.90 (3H, s, CH₃O-7), a methyl group at δ_H 2.39 (3H, s, CH₃-2), three methylenes at δ_H 4.39 (2H, s, H-1′), δ_H 3.80

(2H, q, *J* =6.1 Hz, H-4′), and 3.21 (2H, t, *J* = 6.3, H-3′), a phenolic hydroxyl group at δ_H 11.40 (1H s, OH-5), and a hydroxyl group at δ_H 5.03 (1H, t, *J* = 5.4 Hz, 1H, OH-4′). Examination of the ^{13}C NMR spectrum (Table 2) revealed 14 carbon signals: a carbonyl group C-4 (δ_C 182.4), the two aromatic carbons C-3 (δ_C 108.9) and C-8 (δ_C 91.3), three non-oxygenated quaternary aromatic carbons at C-8a (δ_C 158.2), C-4a (δ_C 104.6), and C-6 (δ_C 101.0), and three oxygenated quaternary aromatic carbons at C-2 (δ_C 168.9), C-5 (δ_C 159.9), and C-7 (δ_C 163.9) and the methylene C-1′ (δ_C 49.3). Analysis of the ^1H and ^{13}C NMR data of **2** revealed the presence of the same 5-hydroxy-4H-chromen-4-one moiety as found in xanthones [18,19].

Table 2. ^1H (500 MHz) and ^{13}C (125 MHz) NMR data of compounds **3–5** in DMSO-d_6.

Position	3		4		5	
	δ_H	δ_C, Type	δ_H	δ_C, Type	δ_H	δ_C, Type
2		168.9, qC		168.7, qC		168.8, qC
3	6.31, s	108.9, CH	6.30, s	108.9, CH	6.29, s	108.9, CH
4		182.4, qC		182.3, qC		182.3, qC
4a		104.6, qC		104.7, qC		104.7, qC
5		159.9, qC		159.1, qC		159.6, qC
6		101.0, qC		101.2, qC		102.3, qC
7		163.9, qC		163.7, qC		163.6, qC
8	6.78, s	91.3, CH	6.76, s	91.1, CH	6.76, s	91.2, CH
8a		158.2, qC		158.2, qC		157.8, qC
1′	4.39, s	49.3, CH₂	4.33, s	49.4, CH₂	3.99, d, (6.7)	48.4, CH₂
3′	3.21, t (6.3)	56.6, CH₂	2.91, s	42.0, CH₃	2.54, s	39.1, CH₃
4′	3.80, q (6.1)	55.3, CH₂				
OH-5	13.40, s					
OH-4′	5.03, t (5.4)					
OCH₃-7	3.90, s	57.2, CH₃	3.90, s	57.2, CH₃	3.90, s	57.2, CH₃
CH₃-2	2.39, s	20.4, CH₃	2.39, s	20.4, CH₃	2.39, s	20.4, CH₃

In the ^1H-^1H COSY spectrum, there were correlations from H-4′ to OH-5′ and H-3′. According to the HMBC, there were correlations from H-1′ to C-6, C-5, and C-7, H-4′ to C-3′, OH-4′ to C-3′. The sulfur atom present in **3** was shown to be attached at C-1′and C-3′, indicated that C-1′was attached at C-6. Further confirmation was found for HMBC correlations of OH-5 to C-4a, C-6, C-5; CH₃-2 to C-3, C-2; CH₃O-7 to C7, H-3 to CH₃-2, C-4a, C-2; H-8 to C-4a, C-6, C-8a, C-7, C-4, a hydroxyl group could be located at C-5, a methoxy groups could be located at C-7, a methyl group could be located at C-2. Selected key correlations in the observed NMR spectrum are shown in Figure 3. On the basis of these results, the structure of compound **3** was established as shown.

Amycolachromone D (**4**) displayed HRESIMS peak at *m/z* 321.0406 [M + Na]⁺ (calcd 321.0409), corresponding to the molecular formula $C_{13}H_{14}O_6S$ (nine degrees of unsaturation). Analysis of the NMR data of **4** (Table 2) revealed for two aromatic protons at δ_H 6.76 (1H, s, H-8), 6.30 (1H, s, H-3), a methoxy groups at δ_H 3.90 (3H, s, CH₃O-7), two methyl groups at δ_H 2.91 (3H, s, H-3′) and 2.39 (3H, s, CH₃-2), a methylene group at δ_H 4.33 (2H, s, H-1′). The ^{13}C NMR (Table 2) revealed 13 carbon signals: a carbonyl group C-4 (δ_C 182.3), two aromatic carbon C-3 (δ_C 108.9) and C-8 (δ_C 91.1), three nonoxygenated quaternary aromatic carbons at C-8a (δ_C 158.2),C-4a (δ_C 104.7), and C-6 (δ_C 101.2), three oxygenated quaternary aromatic carbons at C-2 (δ_C 168.7), C-5 (δ_C 159.1), and C-7 (δ_C 163.7), a methoxy groups CH₃O-7 (δ_C 57.2), two methyl groups C-3′ (δ_C 42.0) and CH₃-2 (δ_C 20.4), a methylene group C-1′ (δ_C 49.4). Analysis of the ^1H and ^{13}C NMR data of **4** revealed the presence of the same 5-hydroxy-4H-chromen-4-one moiety as found in xanthones [18,19]. A side-by-side comparison of the NMR spectroscopic data with those of **3** showed them to be nearly identical except for the final hydroxymethyl unit on the side chain.

According to the HMBC correlations from H-1′ to C-6, C-5 and C-7, the sulfur atom present in **4** was shown to be attached at C-1′and C-3′, indicating that C-1′ was attached at C-6, Further confirmation was found for HMBC correlations of CH₃O-7 to C7; H-3 to

CH$_3$-2, C-4a, C-2; H-8 to C-4a, C-6, C-8a, C-7, C-4, a methoxy group could be located at C-7 and a methyl group could be located at C-2. Selected key correlations in the observed NMR spectrum are shown in Figure 3. On the basis of these results, the structure of compound **4** was established as shown.

Amycolachromone E (**5**) displayed HRESIMS peak at *m/z* 305.0462 [M + Na]$^+$ (calcd 305.0460), corresponding to the molecular formula C$_{13}$H$_{14}$O$_5$S (eight degrees of unsaturation). Analysis of the NMR data of **5** (Table 2) revealed for two aromatic protons at δ_H 6.76 (1H, s, H-8), 6.29 (1H, s, H-3), a methoxy groups at δ_H 3.90 (3H, s, CH$_3$O-7), two methyl groups at δ_H 2.54 (3H, s, H-3′) and 2.39 (3H, s, CH$_3$-2) and a methylene group at δ_H 3.99 (2H, d, *J* = 6.7 Hz, H-1′). The ^{13}C NMR (Table 2) revealed 13 carbon signals: a carbonyl group C-4 (δ_C 182.3), two aromatic carbon C-3 (δ_C 108.9) and C-8 (δ_C 91.2), three nonoxygenated quaternary aromatic carbons at C-8a (δ_C 157.8), C-4a (δ_C 104.7), and C-6 (δ_C 102.3), three oxygenated quaternary aromatic carbons at C-2 (δ_C 168.8), C-5 (δ_C 159.6), and C-7 (δ_C 163.6), a methoxy groups CH$_3$O-7 (δ_C 57.2), two methyl groups C-3′ (δ_C 39.1) and CH$_3$-2 (δ_C 20.4), a methylene group C-1′ (δ_C 48.4). Analysis of the ^{1}H and ^{13}C NMR data of **5** revealed the presence of the same 5-hydroxy-4H-chromen-4-one moiety as found in xanthones [18,19]. A side-by-side comparison of the NMR spectroscopic data with those of **3** showed them to be nearly identical except for the final sulfur monoxide unit on the side chain.

According to the HMBC correlations from H-1′ to C-6, C-5 and C-7, H-3′ to C-1′, the sulfur atom present in **5** was shown to be attached at C-1′and C-3′, indicating that C-1′ was attached at C-6, Further confirmation was found for HMBC correlations of CH$_3$O-7 to C7; H-3 to CH$_3$-2, C-4a, C-2; H-8 to C-4a, C-6, C-8a, C-7 and C-4, a methoxy group could be located at C-7, a methyl group could be located at C-2. Selected key correlations in the observed NMR spectrum are shown in Figure 3. On the basis of these results, the structure of compound **5** was established as shown.

Amycolachromone F (**6**), $[\alpha]_D^{25}$ −54 (*c* 0.1, MeOH), displayed HRESIMS peak at *m/z* 337.0915 [M + H]$^+$ (calcd 337.0923), corresponding to the molecular formula C$_{16}$H$_{16}$O$_8$ (nine degrees of unsaturation). Analysis of the ^{1}H data of **6** (Table 3) revealed resonance for three aromatic protons at δ_H 7.52 (1H, t, *J* = 8.3 Hz, H-3), 6.60 (1H, d, *J* = 8.3 Hz, H-4), 6.53 (1H, d, *J* = 8.3 Hz, H-2), a methoxy group at δ_H 3.50 (3H, s, H-15), a methyl group at δ_H 1.06 (3H, d, *J* = 6.4 Hz, H-16), a methylene at δ_H 2.81 (1H, dd, *J* = 14.4, 12.9 Hz, H-9a) and 2.25 (1H, dd, *J* = 14.5, 5.3 Hz, H-9b), a oxygenated methine at δ_H 4.20 (1H, dd, *J* = 10.5, 6.0 Hz, H-7), a methine at δ_H 1.97–1.86 (1H, m, H-8), three hydroxyl groups at δ_H 11.35 (1H s, OH-1), 8.09 (1H, s, OH-11), and 5.91 (1H, d, *J* = 6.0 Hz, OH-7). The ^{13}C NMR (Table 3) revealed sixteen carbon signals: three carbonyl group C-10 (δ_C 198.6), C-12 (δ_C 191.8) and C-14 (δ_C 168.5), three aromatic carbon C-3 (δ_C 138.7), C-2 (δ_C 109.5), and C-4 (δ_C 107.4), a nonoxygenated quaternary aromatic carbons at C-13 (δ_C 106.5), two oxygenated quaternary aromatic carbons at C-1 (δ_C 161.9) and C-5 (δ_C 158.9), two sp^3-quaternary carbon C-11 (δ_C 90.0) and C-6 (δ_C 73.0), a methoxy group C-15 (δ_C 52.7), a methyl group C-16 (δ_C 18.6), an oxygenated methine C-7 (δ_C 71.8), a methine C-8 (δ_C 31.1) and a methylene C-9 group (δ_C 43.1). Analysis of the ^{1}H and ^{13}C NMR data of **6** revealed the presence of the same 5-hydroxy-4H-chromen-4-one moiety as found in xanthones [18,19]. In the ^{1}H-^{1}H COSY spectrum, the correlations from H-7 to H-8 and OH-7, from H-8 to H-9 and H-16. Further confirmation was found for HMBC correlations of H-7 to C-16, C-6, C-11 and C-9; H$_3$-16 to C-7, C-8 and C-9, indicated that C-16 was attached to C-8, and OH-7 was located at C-7. HMBC correlations from the O-methyl proton signal H$_3$-15 to the carboxylic carbon C-14 confirmed that the O-methyl group was located at C-14. HMBC correlations from OH-11 to C-11, C-6 and C-10, OH-1 to C-2, C-13 and C-1 indicated that OH-1 and OH-11 were attached to C-1 and C-11, respectively [22,23]. Selected key correlations in the observed NMR spectrum are shown in Figure 3. Thus, the planar structure of **6** was established. Moreover, the relative configuration of **6** was established to be 6R*, 7S*, 8R* and 11R* by X-ray crystallography using Mo K*a* radiation (Figure 4).

**Table 3.** ^{1}H (500 MHz) and ^{13}C (125 MHz) NMR data of compound **6** in DMSO-d_6.

Position	6	
	δ_{H}	δ_{C}, Type
1		161.9, qC
2	6.53, d (8.3)	109.5, CH
3	7.52, t (8.3)	138.7, CH
4	6.60, d (8.3)	107.4, CH
5		158.9, qC
6		73.0, qC
7	4.20, dd (10.5, 6.0)	71.8, CH
8	1.97–1.86, m	31.1, CH
9	2.81, dd (14.4, 12.9); 2.25 dd(14.5, 5.3)	43.1, CH$_2$
10		198.6, qC
11		90.0, qC
12		191.8, qC
13		106.5, qC
14		168.5, qC
15	3.50, s	52.7, CH$_3$
16	1.06, d (6.4)	18.6, CH$_3$
OH-1	11.35, s	
OH-7	5.91, d (6.0)	
OH-11	8.09, s	
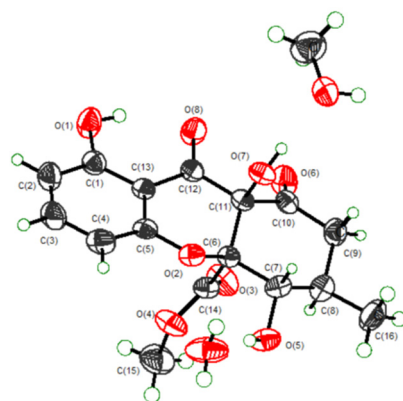
Figure 4. ORTEP diagram for the single-crystal X-ray of Amycochromone F (**6**).

Further analysis of the structures allowed us to raise a plausible biosynthetic pathway of compounds **1**–**6**. As outlined in the Scheme 1, compounds **1**–**5** were structurally related to the known metabolite 6-methoxymethyleugenin, which was derived from the widely existing 5,7-dihydroxy-2-methylchromone via the hydroxymethylation with formaldehyde and the methylation with SAM (*S*-adenosyl methionine). The compound **1** was the dimerization of 6-methoxymethyleugenin, and the sequential methylation with SAM could afford the related compound **2**. For compound **3**–**5**, we proposed that the sulfur in these structures was from L-cysteine. Thus, the Michael addition of L-cysteine to the *ortho*-quinone methide intermediate from 6-methoxymethyleugenin gave the compound **I**. Then, transamination, decarboxylation and reduction sequence of **I** furnished the 2-sulfo-ethanol **II** occurred. An oxidation of sulfur in **II** gave the compound **III**. Finally, compound **3** was obtained through the double oxidation of sulfur in **II**. The oxidation of the hydroxyl group in **III** to the corresponding carboxylic acid occurred and followed with a decarboxylation afforded for compound **5**. Furthermore, compound **4** was the oxidation product of **5** [24,25]. In addition, compound **6** was the oxidation product of the known natural product blennolide B, which was proposed by Franck to be a derivative of emodin (Scheme 2) [26].
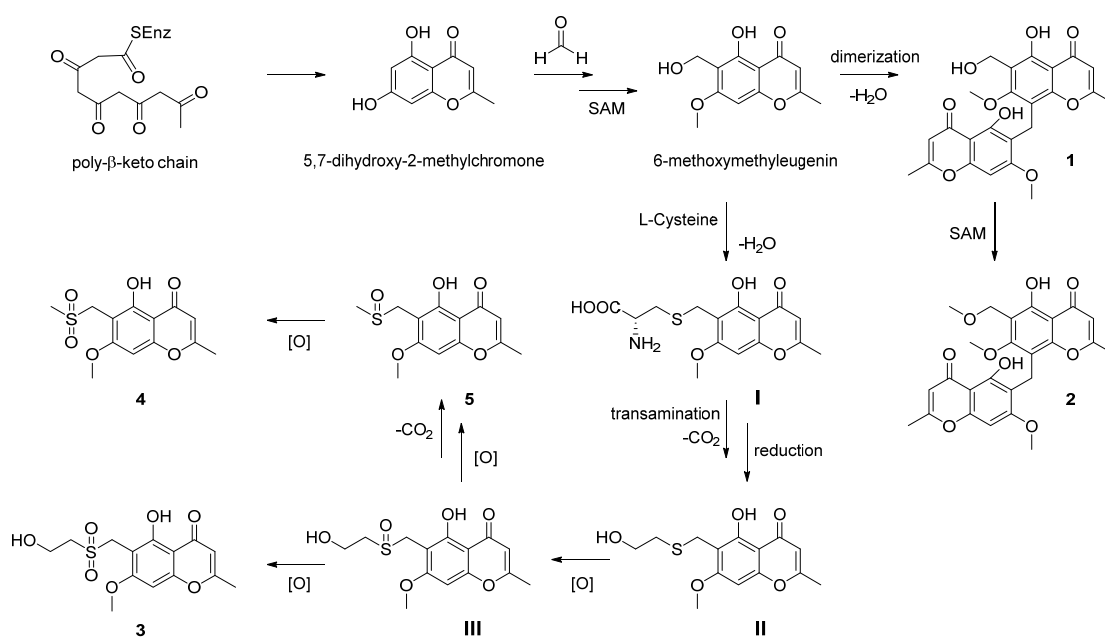
Scheme 1. Proposed hypothetical biosynthesis pathway of **1–5**.
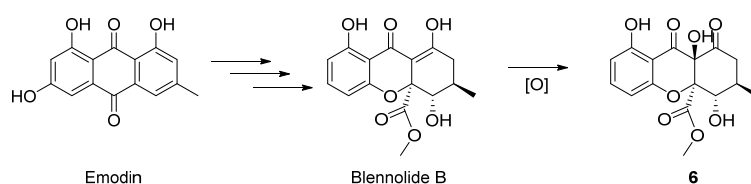
Scheme 2. Proposed hypothetical biosynthesis pathway of **6**.

The structures of five known compounds were identified as 6-ethoxymethyleugenin (**7**), 6-methoxymethyleugenin (**8**), 6-hydroxymethyleugenin (**9**), emodin (**10**) and the ascomycete metabolite chaetoquadrin D (**11**) by comparison of spectroscopic data with reported values and are described here for the first time as produced by *Amycolatopsis* sp.

The AlkB family of DNA repair enzymes utilize an α-ketoglutarate/Fe(II)-dependent mechanism to oxidize the aberrant alkyl groups, finally repairing alkyl DNA bases [27,28]. Compounds **1–11** were evaluated for their in vitro ABH2 inhibitory activities. Compounds **1–11** exhibited weak inhibitory activity against the ABH2 enzyme. However, in 2019, a paper was published that tested emodin (**10**). It exhibited strong inhibitory activity for the ALKH3 enzyme with IC$_{50}$ of 8.8 μM [29]. This hinted that these compounds might inhibit other members of the AlkB family of enzymes.

In conclusion, the chemical investigation of a streptomycin-resistant strain of the deep-sea marine actinomycete, *Amycolatopsis* sp. WP1, led to the isolation and identification of six novel compounds, amycolachromones A–F (**1–6**) and five known analogues (**7–11**). Among them, amycolachromones A–B (**1–2**) represents an unusual fused skeleton between two 6-hydroxymethyleugenin, and the relative configuration of amycolachromones F (**6**) was determined by the signal-crystal X-ray diffraction. The discovery of amycolachromones A–F not only expanded the chemical diversity of natural products and inspire further synthetic studies, but also provided a template for the exploration of inhibitors of other members of the AlkB family of enzymes.

3. Materials and Methods

General experimental procedures. All chemical reagents and solvents were purchased from Sigma–Aldrich (Shanghai, China). UV spectra were acquired with a DU 800 UV/vis spectrophotometer (Beckman Coulter, Brea, CA, USA). IR spectra were acquired with a

Nicolet 380 FT-IR (Thermo Electron Corporation, Beverly, MA, USA). NMR experiments were conducted using an Agilent NMR 500 MHz spectrometer (Santa Clara, CA, USA) and BRUKER NMR 600 MHz spectrometer (San Jose, CA, USA) with $(CD_3)_2SO$ as the solvent (referenced to residual DMSO at δ_H 2.54 and δ_C 39.5) at 25 °C. Electrospray ionization mass spectra (ESIMS) were acquired using an AB Sciex TripleTOF 4600 spectrometer (Boston, MA, USA) in the positive and negative ion mode. HPLC experiments were performed on a Hitachi Elite LaChrom system (Tokyo, Japan) equipped with a diode array detector model L-2450, pump L-2130 and autosampler L-2200. Semipreparative HPLC experiments were completed with a Waters XBridge Prep C_{18} (Miflord, CO, USA) 5 μm, 10 mm × 250 mm column and Phenomenex Luna C_{18} 5 μm, 250 mm × 21.2 mm column.

Bacterial Strain and Culture Conditions. The WP1 strain (CGMCC No. 10738) was isolated from deep-sea sediments of the Southwest Indian Ocean and identified as *Amycolatopsis* sp. by 16S rRNA sequence comparison. WP1 was grown in ISP_2 medium consisting of 1.0% (*w/v*) malt extract, 0.4% (*w/v*) yeast extract, 0.4% (*w/v*) glucose and 3% (*w/v*) sea salt, the pH of medium was adjusted to 7.4 using 2 M HCl and 2 M NaOH.

Mutants of strain WP1. The WP1 strain suspensions were spread onto ISP_2 plates containing different concentrations (0, 10, 20, 30, 40, 50 and 60 mg/mL) of streptomycin. The plates were incubated at 37 °C for 7 days. Mutant colonies producing the white pigment different than the WP1 strain were selected, generating mutant strain L-30-6, which was obtained on the IPS_2 plate containing 30 mg/mL streptomycin.

Extraction and isolation. The mutant L-30-6 strain was inoculated into ISP_2 broth with 3% sea salt in 250 mL Erlenmeyer flasks, at 30 °C on a rotary shaker at 180 rpm for 2 days as seed culture. Each of the seed cultures (32 mL) was transferred into 1 L Erlenmeyer flasks containing 400 mL of ISP_2 supplemented with 3% sea salt. These flasks were incubated at 30 °C on a rotary shaker at 180 rpm for 6 days. The resulting cultures (60 L) were centrifuged to yield the supernatant and a mycelial pellet. The supernatant was adsorbed onto macroporous resin XAD16N (DOW, St. Louis, Missouri, CA, USA) and eluted with linear gradient of 0–100% EtOH in H_2O to afford six fractions (A–F).

Fraction C (3.8 g) was subjected to semipreparative HPLC (Phenomenex Luna C_{18}, 250 mm × 21.2 mm, 5 μm, 10 mL/min) using a gradient solvent from 40–90% MeOH in H_2O over 30 min to give five fractions (C1–C5). Fraction C2 was further purified by semipreparative HPLC (Waters XBridge Prep C_{18} 5 μm, 10 mm× 250 mm, 4 mL/min) using an isocratic solvent system of $CH_3CN:H_2O$ (15:85) over 30 min to afford compound **6** (10.2 mg) and C2A. Subfraction C2A was further purified by preparative HPLC with MeOH-H_2O (45:55) to provide compound **7** (2.6 mg). Fraction C3 was further purified by semipreparative HPLC with MeOH-H_2O (45:55) to yield compound **12** (6.5 mg), **3** (3.1 mg) and **4** (2.2 mg). Fraction C4 was further purified by semipreparative HPLC with MeOH:H_2O (45:55) to afford compound **5** (2.2 mg).

Fraction D (2.1 g) was subjected to semipreparative HPLC (Phenomenex Luna C18, 250 mm × 21.2 mm, 5 μm, 10 mL/min) using a gradient solvent from 50–80% MeOH in H_2O over 30 min to generate five fractions (D1–D5). Fraction D3 was further purified by semipreparative HPLC using an isocratic solvent system of MeCN:H_2O (50:50) to afford compound **1** (1.7 mg) and compound **2** (1.8 mg). D4 was subjected to preparative HPLC with MeCN:H_2O (30:70) to provide compounds **9** (35.3 mg) and **10** (13.5 mg). D5 was further purified by preparative HPLC with MeOH-H_2O (45:55) to yield compounds **8** (1.9 mg) and **11** (6.8 mg). The following are details of the extraction and isolation of the compounds.

Amycolachromone A (**1**): White, amorphous powder; UV (MeOH) λmax (log ε) 253 (3.28) nm; IR (ZnSe) ν_{max} 3426, 3195, 2844, 1656, 1445, 1008 cm^{-1}; ^1H and ^{13}C NMR data, Table 1; HRESIMS *m/z* 477.1172 $[M + Na]^+$ (calcd for $C_{24}H_{22}O_9$, 477.1162).

Amycolachromone B (**2**): White, amorphous powder; UV (MeOH) λmax (log ε) 254 (3.46) nm; IR (ZnSe) ν_{max} 3460, 3190, 2894, 1658, 1445, 1008 cm^{-1}; ^1H and ^{13}C NMR data, Table 1; HRESIMS *m/z* 469.1502 $[M + H]^+$ (calcd for $C_{25}H_{24}O_9$, 469.1499), *m/z* 491.1333 $[M + Na]^+$ (calcd 469.1318).

Amycolachromone C (**3**): White, amorphous powder; UV (MeOH) λmax (log ε) 250 (3.43), 233 (3.46) nm; IR (ZnSe) ν_{max} 3420, 3199, 2993, 1650, 1310, 1089 cm^{-1}; ^{1}H and ^{13}C NMR data, Table 2; HRESIMS m/z 351.0515 [M + Na]$^+$ (calcd for $C_{14}H_{16}O_7S$, 351.0514).

Amycolachromone D (**4**): White, amorphous powder; UV (MeOH) λmax (log ε) 250 (3.56), 233 (3.58) nm; IR (ZnSe) ν_{max} 3520, 32,469, 2990, 1750, 1281, 1008 cm^{-1}; ^{1}H and ^{13}C NMR data, Table 2; HRESIMS m/z 321.0406 [M + Na]$^+$ (calcd for $C_{13}H_{14}O_6S$, 321.0409).

Amycolachromone E (**5**): White, amorphous powder; UV (MeOH) λmax (log ε) 250 (3.61), 240 (3.61) nm; IR (ZnSe) ν_{max} 3470, 3122, 2880, 1603, 1210, 1089 cm^{-1}; ^{1}H and ^{13}C NMR data, Table 2; HRESIMS m/z 305.0462 [M + Na]$^+$ (calcd for $C_{13}H_{14}O_5S$, 305.0460).

Amycolachromone F (**6**): White, crystal; UV (MeOH) λmax (log ε) 356 (3.20), 277 (3.68) nm; IR (ZnSe) ν_{max} 3477, 2956, 2916, 1748, 1622, 1475, 1349, 1083 cm^{-1}; ^{1}H and ^{13}C NMR data, Table 3; HRESIMS m/z 337.0915 [M + H]$^+$ (calcd for $C_{16}H_{16}O_8$, 337.0923).

6-Ethoxymethyleugenin (**7**): White, amorphous powder; HR-ESIMS m/z 287.0891 [M + Na]$^+$ (calcd for $C_{14}H_{16}O_5$, 287.0985). ^{1}H-NMR (600 MHz, DMSO-d_6): δ_H 13.19 (s, OH-5), 6.70 (s, 1H, H-8), 6.28 (s, 1H, H-3), 4.41 (s, 2H, CH_2OCH_3), 3.89 (s, 3H, OCH$_3$), 3.44 (q, J = 7.0 Hz, 2H, 6-CH$_2$OCH_2), 2.40 (s, 3H, 2-CH$_3$), 1.08 (t, J = 7.0 Hz, 3H, OCH$_2$CH_3). ^{13}C-NMR (150 MHz, DMSO-d_6): δ_C 182.6 (C-4), 168.5 (C-2), 164.3 (C-7), 159.9 (C-5), 158.0 (C-8a), 109.1 (C-3), 108.9 (C-6), 104.4 (C-4a), 89.6 (C-8), 65.1 (CH$_2$OCH$_3$), 59.3 (6-CH$_2$OCH$_2$), 56.9 (7-OCH$_3$), 20.4 (2-CH$_3$) and 15.3 (CH$_2$CH$_3$).

6-Methoxymethyleugenin (**8**): White, amorphous powder; HR-ESIMS m/z 273.0738 [M + Na]$^+$ (calcd for $C_{13}H_{14}O$, 273.0739). ^{1}H-NMR (600 MHz, CDCl$_3$): δ_H 13.04 (s, OH-5), 6.36 (s, 1H, H-8), 6.04 (s, 1H, H-3), 4.55 (s, 2H, CH_2OCH_3), 3.90 (s, 3H, OCH$_3$), 3.40 (s, 3H, CH$_2$OCH_3), 2.35 (s, 3H, CH$_3$). ^{13}C-NMR (150 MHz, CDCl$_3$): δ_C 182.4 (C-4), 166.6 (C-2), 164.2 (C-7), 160.6 (C-5), 158.2 (C-8a), 109.1 (C-3), 108.9 (C-6), 105.1 (C-4a), 89.6 (C-8), 61.6 (CH$_2$OCH$_3$), 58.2 (CH$_2$OCH$_3$), 56.2 (OCH$_3$) and 20.4 (2-CH$_3$).

6-Hydroxymethyleugenin (**9**): White, amorphous powder; HRESIMS m/z 259.0579 [M + Na]$^+$ (calcd for $C_{12}H_{12}O_5$, 259.0582). ^{1}H-NMR (600 MHz, DMSO-d_6): δ_H 13.09 (s, OH-5), 6.65 (s, 1H, H-8), 6.24 (s, 1H, H-3), 4.55 (t, J = 5.3 Hz, CH$_2$OH), 4.43 (d, J = 5.2 Hz, 2H, H-9), 3.87 (s, 3H, OCH$_3$), 2.38 (s, 3H, CH$_3$). ^{13}C-NMR (150 MHz, DMSO-d_6): δ_C 182.5 (C-4), 168.4 (C-2), 164.1 (C-7), 159.1 (C-5), 157.7 (C-8a), 112.5 (C-6), 08.8 (C-3), 104.6 (C-4a), 90.7 (C-8), 56.7 (OCH$_3$), 50.9 (CH$_2$OH) and 20.4(CH$_3$).

Emodin (**10**): White, amorphous powder; HRESIMS m/z 269.0448 [M − H]$^-$ (calcd for $C_{15}H_{12}O_5$, 269.0450). ^{1}H-NMR (500 MHz, DMSO-d_6): δ_H 12.07 (d, J = 19.5 Hz, 2H, OH), 7.49 (d, J = 1.1 Hz, 1H, H-5), 7.16 (s, 1H, H-7), 7.10 (d, J = 2.4 Hz, 1H, H-4), 6.57 (d, J = 2.4 Hz, 1H, H-2), 2.41 (s, 3H, CH$_3$). ^{13}C-NMR (150 MHz, DMSO-d_6): δ_C 190.0 (C-9), 182.0 (C-10), 166.6 (C-6), 165.0 (C-8), 161.9 (C-1), 148.6 (C-3), 135.6 (C-10a), 133.3 (C-4a), 24.6 (C-2), 120.9 (C-4), 113.9 (C-9a), 109.6 (C-5), 109.2 (C-7), 108.4 (C-8a) and 22.0 (CH$_3$).

Chaetoquadrin D (**11**): White, amorphous powder; HRESIMS m/z HR-ESIMS m/z 370.0969 [M + H]$^+$ (calcd for $C_{16}H_{19}NO_7S$, 370.0960). ^{1}H-NMR (500 MHz, DMSO-d_6): δ_H 13.43 (s, 5-OH), 8.08 (t, NH), 6.79 (s, H-8), 6.32 (s, H-3), 4.36 (s, H-1′), 3.92 (s, 7-OCH$_3$), 3.45 (dd, J = 13.6, 6.1 Hz, H-4′), 3.20 (t, J = 7.0 Hz, H-3′), 2.41 (s, 2-CH$_3$), 1.81 (s, H-7′). ^{13}C-NMR (125 MHz, DMSO-d_6): δ_C 182.4 (C-4), 70.1 (C-6′), 169.0 (C-2), 163.7 (C-7), 159.9 (C-5), 158.2 (C-8a), 108.9 (C-3), 104.5 (C-4a), 100.8 (C-6), 91.4 (C-8), 57.3 (7-OCH$_3$), 52.9 (C-3′), 48.5 (C-1′), 32.9 (C-4′), 22.9 (C-7′) and 20.42 (2-CH$_3$).

X-ray Crystallographic Analysis of Compound **6**. Crystals of **6** were obtained in the mixed solvent comprising MeOH and H$_2$O, and crystallographic data were deposited at the Cambridge Crystallographic Data Centre (CCDC) under the reference number CCDC 1873441. The X-ray diffraction data were collected with Mo Kα radiation (λ = 0.71073 Å). The structure was solved by direct methods using the SHELXS-97 program. Orthorhombic $C_{16}H_{16}O_8$, CH$_4$O, H$_2$O, a = 7.7760(3) Å, b = 8.6993(4) Å, c = 26.8196(11) Å, α = 90°, β = 90°, γ = 90°, V = 1814.23(13) Å3, Z = 4, ρCalcd = 1.414 g/cm^3, μ = 0.118 mm^{-1}, and F (0 0 0) = 816. Measurements were in the range 3.038° ≤ θ ≤ 26.368°, with 3697 independent reflections, of which 3133 unique reflections with I > 2σ (I) were collected for the analysis,

Rint = 0.0332. The final R indices: R1 = 0.0455, wR2 = 0.1177 [I > 2σ(I)], R indices (all data): R1 = 0.0566, wR2 = 0.1256, and largest difference peak and hole: 0.560 and-0.231 e Å-3.

The ABH2 family DNA repair enzyme assay. Effects of compounds **1–11** on the ABH2 family demethylase activity reactions on m3c-ss-DNA were evaluated. All reactions were performed at 37 °C in reaction buffer [5 μM Fe(NH$_4$)$_2$(SO$_4$)$_2$, 0.93 mMα-ketoglutarate, 1.86 mM ascorbic acid, and 46.56 mM HEPES (pH 8.0)] for 1 h. Varying concentrations of compounds **1–11** (0, 5.0, 7.5, 20, 30, 40, 50, 75 and 100 μM) were used for tests. The m3c-ss-DNA was pre-mixed with reaction buffer in a concentration of 5.0 μM. The reactions were initiated by adding 2.0 μM ABH2. The reactions were stopped by adding 10.0 mM EDTA followed by heating to 95 °C for 5 min. All the results of reaction were analyzed by HPLC. All reaction samples were quantified by DNApac PA-100 column (4 mm × 250 mm, Thermo Scientific, (Waltham, MA, USA) with isocratic 60 % mobile B, 1.5 M ammonium acetate, under a constant flow rate of 1.0 mL/min. Mobile A was water. The UV detection wavelength was 260 nm.

Supplementary Materials: The following supporting information can be downloaded at: https://www.mdpi.com/article/10.3390/md20030162/s1. Figures S1–S35: 1D and 2D NMR, HRESI mass spectra, and crystal data for compounds **1–6**. Table S1. Crystallographic data for Amycochromone F (**6**).

References

1. Blunt, J.W.; Copp, B.R.; Keyzers, R.A.; Munro, M.H.G.; Prinsep, M.R. Marine Natural Products. *Nat. Prod. Rep.* **2017**, *34*, 235–294. [CrossRef] [PubMed]
2. Blunt, J.W.; Copp, B.R.; Keyzers, R.A.; Munro, M.H.; Prinsep, M.R. Marine Natural Products. *Nat. Prod. Rep.* **2016**, *33*, 382–431. [CrossRef] [PubMed]
3. Blunt, J.W.; Copp, B.R.; Keyzers, R.A.; Munro, M.H.; Prinsep, M.R. Marine Natural Products. *Nat. Prod. Rep.* **2015**, *32*, 116–211. [CrossRef]
4. Nutzmann, H.W.; Reyes-Dominguez, Y.; Scherlach, K.; Schroeckh, V.; Horn, F.; Gacek, A.; Schumann, J.; Hertweck, C.; Strauss, J.; Brakhage, A.A. Bacteria-induced Natural Product Formation in the Fungus *Aspergillus nidulans* Requires Saga/Ada-mediated Histone Acetylation. *Proc. Natl. Acad. Sci. USA* **2011**, *108*, 14282–14287. [CrossRef]
5. Bentley, S.D.; Chater, K.F.; Cerdeno-Tarraga, A.M.; Challis, G.L.; Thomson, N.R.; James, K.D.; Harris, D.E.; Quail, M.A.; Kieser, H.; Harper, D.; et al. Complete Genome Sequence of the Model Actinomycete *Streptomyces coelicolor* A3(2). *Nature* **2002**, *417*, 141–147. [CrossRef]
6. Nett, M.; Ikeda, H.; Moore, B.S. Genomic Basis for Natural Product Biosynthetic Diversity in the Actinomycetes. *Nat. Prod. Rep.* **2009**, *26*, 1362–1384. [CrossRef]
7. Bode, H.B.; Bethe, B.; Hofs, R.; Zeeck, A. Big Effects from Small Changes: Possible Ways to Explore Nature's Chemical Diversity. *Chembiochem* **2002**, *3*, 619–627. [CrossRef]
8. Chen, J.; Zhang, H.; Ye, X.; Wei, B.; Emam, M.; Zhang, H.; Wang, H. The Structural Diversity of Marine Microbial Secondary Metabolites Based on Co-Culture Strategy: 2009–2019. *Mar. Drugs* **2020**, *18*, 449. [CrossRef]
9. Henrikson, J.C.; Hoover, A.R.; Joyner, P.M.; Cichewicz, R.H. A Chemical Epigenetics Approach for Engineering the in Situ Biosynthesis of a Cryptic Natural Product from *Aspergillus niger*. *Org. Biomol. Chem.* **2009**, *7*, 435–438. [CrossRef]

10. Ochi, K.; Hosaka, T. New strategies for drug discovery: Activation of silent or weakly expressed microbial gene clusters. *Appl. Microbiol. Biotechnol.* **2013**, *97*, 87–98. [CrossRef]

11. Ochi, K.; Tanaka, Y.; Tojo, S. Activating the Expression of Bacterial Cryptic Genes by *rpoB* Mutations in RNA Polymerase or by Rare Earth Elements. *J. Ind. Microbiol. Biotechnol.* **2014**, *41*, 403–414. [CrossRef]

12. Shima, J.; Hesketh, A.; Okamoto, S.; Kawamoto, S.; Ochi, K. Induction of Actinorhodin Production by *rpsL* (Encoding Ribosomal Protein S12) Mutations that Confer Streptomycin Resistance in *Streptomyces lividans* and *Streptomyces coelicolor* A3(2). *J. Bacteriol.* **1996**, *178*, 7276–7284. [CrossRef]

13. Fdhila, F.; Vazquez, V.; Sanchez, J.L.; Riguera, R. DD-diketopiperazines: Antibiotics Active against *Vibrio anguillarum* Isolated from Marine Bacteria Associated with Cultures of *Pecten maximus*. *J. Nat. Prod.* **2003**, *66*, 1299–1301. [CrossRef]

14. Zhang, Y.; Huang, H.; Xu, S.; Wang, B.; Ju, J.; Tan, H.; Li, W. Activation and Enhancement of Fredericamycin A production in Deepsea-derived *Streptomyces somaliensis* SCSIO ZH66 by Using Ribosome Engineering and Response Surface Methodology. *Microb. Cell Fact.* **2015**, *14*, 64. [CrossRef]

15. Fu, P.; Jamison, M.; La, S.; MacMillan, J.B. Inducamides A-C, Chlorinated Alkaloids from an RNA Polymerase Mutant Strain of *Streptomyces* sp. *Org. Lett.* **2014**, *16*, 5656–5659. [CrossRef]

16. Gaspar, A.; Matos, M.J.; Garrido, J.; Uriarte, E.; Borges, F. Chromone: A Valid Scaffold in Medicinal Chemistry. *Chem. Rev.* **2014**, *114*, 4960–4992. [CrossRef]

17. Reis, J.; Gaspar, A.; Milhazes, N.; Borges, F. Chromone as a Privileged Scaffold in Drug Discovery: Recent Advances. *J. Med. Chem.* **2017**, *60*, 7941–7957. [CrossRef]

18. Sumarah, M.W.; Puniani, E.; Blackwell, B.A.; Miller, J.D. Characterization of Polyketide Metabolites from Foliar Endophytes of *Picea glauca*. *J. Nat. Prod.* **2008**, *71*, 1393–1398. [CrossRef]

19. Zhang, F.; Li, L.; Niu, S.; Si, Y.; Guo, L.; Jiang, X.; Che, Y. A Thiopyranchromenone and Other Chromone Cerivatives from an *Endolichenic fungus*, *Preussia africana*. *J. Nat. Prod.* **2012**, *75*, 230–237. [CrossRef]

20. Tuntiwachwuttikul, P.; Phansa, P.; Pootaeng-On, Y.; Taylor, W.C. Chromones from the Branches of *Harrisonia perforata*. *Chem. Pharm. Bull.* **2006**, *54*, 44–47. [CrossRef]

21. Feng, Y.J.; Blunt, J.W.; Cole, A.L.J.; Munro, M.H.G. The Isolation of Two New Chromone Derivatives from the New Zealand fungus *Tolypocladium extinguens*. *J. Nat. Prod.* **2002**, *65*, 1681–1682. [CrossRef] [PubMed]

22. Yong, K.; Kaleem, S.; Yi, W.W.; Wu, B.; Zhang, Z.Z. New Polyhydroxanthones from the Marine-Associated Fungus *Penicillium* sp. ZZ1750. *Tetrahedron Lett.* **2021**, *81*, 153354. [CrossRef]

23. El-Elimat, T.; Raja, H.A.; Day, C.S.; McFeeters, H.; McFeeters, R.L.; Oberlies, N.H. α-Pyrone derivatives, Tetra/Hexahydroxanthones, and Cyclodpsipeptides from Two Freshwater Fungi. *Bioorg. Med. Chem.* **2017**, *25*, 795–804. [CrossRef] [PubMed]

24. Qin, T.; Porco, J.A., Jr. Total Syntheses of Secalonic Acids A and D. *Angew. Chem. Int. Ed. Engl.* **2014**, *53*, 3107–3110. [CrossRef]

25. Qin, T.; Iwata, T.; Ransom, T.T.; Beutler, J.A.; Porco, J.A., Jr. Syntheses of Dimeric Tetrahydroxanthones with Varied Linkages: Investigation of "Shapeshifting" Properties. *J. Am. Chem. Soc.* **2015**, *137*, 15225–15233. [CrossRef]

26. Franck, B.; Stöckigt, J.; Zeidler, U.; Franckowiak, G. Stereospezifische Synthese der 10-Methyl-10-desmethoxycarbonyl-hemisecalonsäure A. *Chem. Ber.* **1973**, *106*, 1198–1220. [CrossRef]

27. Chen, F.; Tang, Q.; Bian, K.; Humulock, Z.T.; Yang, X.; Jost, M.; Drennan, C.L.; Essigmann, J.M.; Li, D. Adaptive Response Enzyme AlkB Preferentially Repairs 1-Methylguanine and 3-Methylthymine Adducts in Double-Stranded DNA. *Chem. Res. Toxicol.* **2016**, *29*, 687–693. [CrossRef]

28. Bian, K.; Chen, F.; Humulock, Z.T.; Tang, Q.; Li, D. Copper Inhibits the alkb Family DNA Repair Enzymes under Wilson's Disease Condition. *Chem. Res. Toxicol.* **2017**, *30*, 1794–1796. [CrossRef]

29. Pilzys, T.; Marcinkowski, M.; Kukwa, W.; Garbicz, D.; Dylewska, M.; Ferenc, K.; Mieczkowski, A.; Kukwa, A.; Migacz, E.; Wolosz, D. ALKBH Overexpression in Head and Neck Cancer: Potential Target for Novel Anticancer Therapy. *Sci. Rep.* **2019**, *9*, 13249. [CrossRef]